

# A Novel Approach for Edge Orientation Determination Based on Pixel Pair Matching

Hou-Chun Ting and Hsueh-Ming Hang

Dept. of Electronics Engineering  
National Chiao Tung University, Hsinchu, Taiwan 300, ROC  
Email: hmhang@cc.nctu.edu.tw

## Abstract

*A novel edge orientation determination algorithm is proposed. It can detect edges and decide very precisely their orientations based on a pixel pair matching technique. Three image edge structure measures, profile diversity, edge convexity and edge continuity, are designed to facilitate the determination process. The basic algorithm outputs an integer-pixel orientation vector for each detected edge and this orientation vector can be refined to subpixel accuracy by a polynomial fitting method. Simulation results are included to show the advantages of this approach.*

## 1 Introduction

Many edge detection techniques have been developed for image processing and computer vision. According to the detection operators used, the edge orientation estimation techniques can be classified into two major groups [1]: (1) employing a pair of orthogonal edge (gradient) operators to detect the directional edge magnitudes of the input image and then apply the inverse tangent formula to the two magnitudes; and (2) correlating the input image with a set of masks (edge detectors) oriented to some selected directions and the edge orientation is determined by the mask having the maximum correlation. In the case of using the detected edge orientation to re-scale or interpolate digital images [2], the accuracy of the detected edge orientation is very critical [3] because a single false edge orientation can lead to catastrophic visible errors in the interpolated image. Different from the above two classes of techniques, a new algorithm is proposed to estimate the edge orientation in this paper.

Let  $\mathcal{I}_{h,\theta}$  be an edge image in the two dimensional

---

This work was supported in part by National Science Council of R.O.C. under Grant NSC86-2213-E-009-064.

continuous image space, as illustrated in Fig. 1. An aperture-sampled discrete edge image can be modeled as

$$I(n_x, n_y) = \int_{n_y w - \frac{w}{2}}^{n_y w + \frac{w}{2}} \int_{n_x w - \frac{w}{2}}^{n_x w + \frac{w}{2}} \mathcal{I}_{h,\theta}(x, y) dx dy, \quad (1)$$

where  $n_x$  and  $n_y$  are the integer coordinates, and  $w$  is the sampling grid length. Three structural features, edge profile diversity, edge convexity and linkage continuity, are devised to use in the edge orientation determination process to reduce the probability of the incorrect edge orientation detection.

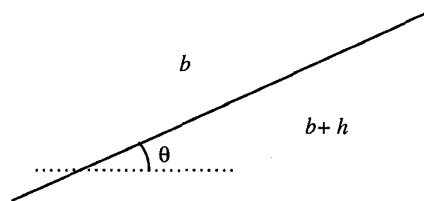


Figure 1: A simple edge model.

This paper is organized as follows. Section 2 defines the three structural feature measures and analyzes the discrete edge model statistically. Based on the statistical analysis, an edge orientation determination method is developed in Section 3 and further refined in Section 4. Section 5 presents the simulation results to show the advantages of the proposed method. Section 6 concludes this paper.

## 2 Statistical Analysis for Discrete Edge Model

Let  $P_1 = \langle I(n_x, n_y), I(n_x - 1, n_y) \rangle$  be an anchor pixel pair and  $P_2 = \langle I(n_x + k, n_y + 1), I(n_x - 1 + k, n_y + 1) \rangle$  be the sliding pixel pair where the integer  $k$  is

the horizontal shift between them. The edge profile diversity of two pixel pairs,  $P_1$  and  $P_2$ , is defined as:

$$d(P_1, P_2) = \|P_1 - P_2\|_\ell + \gamma \cdot |\nabla P_1 - \nabla P_2|, \quad (2)$$

where  $\|\cdot\|_\ell$  is the  $\ell$ -norm,  $\nabla$  is the gradient, and  $\gamma$  is an adjustable weighting factor which is taken to be 1 in this study.  $d(P_1, P_2)$  is an indication of the similarity between  $P_1$  and  $P_2$  including a rough measure of their shapes (slopes). For example, two parallel best-matched pixel pairs straddle the same edge should have the minimum profile diversity.

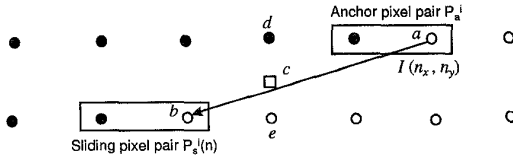


Figure 2: An example of the convexity measure with  $i = 0$ ,  $j = -2$  and  $k = -3$ .

Next, we invent the convexity measure to exclude the matched pixel pairs which do not straddle the same edge. Fig. 2 shows an example which illustrates this situation. Based on our observations on the edge image, we suggest the following proposition. The convexity constraint demands the pixel value  $c$  being inside the range of  $d$  and  $e$ ; that is,  $c \in [\min\{d, e\}, \max\{d, e\}]$ . We thus have

$$c = \alpha d + (1 - \alpha)e \quad \text{or} \quad c = (1 - \beta)d + \beta e, \quad (3)$$

where  $\alpha + \beta = 1$  and  $0 \leq \alpha, \beta \leq 1$ . By manipulating (3), we have  $\alpha - \beta = \frac{2c - d - e}{d - e}$ . To satisfy the convexity constraint, the four pixels should comply with the following requirement:  $0 \leq \frac{2c - d - e}{d - e} \leq 1$ . If  $c$  is taken the average of  $a$  and  $b$ , and substitute the variables by the pixel values, we have

$$\begin{aligned} N_v(P_1, P_2) &= |I(n_x - i, n_y) + I(n_x - i + k, n_y + 1) - \\ &\quad I(n_x - i + j, n_y) - I(n_x - i + j, n_y + 1)|, \end{aligned} \quad (4)$$

and

$$D_v(P_1, P_2) = |I(n_x - i + j, n_y) - I(n_x - i + j, n_y + 1)|, \quad (5)$$

where  $i = 0, 1$  and  $1 \leq j < k$  if  $k > 0$  (or  $k < j \leq -1$  if  $k < 0$ ). The convexity measure is defined as

$$v(P_1, P_2) = \max_{i=0,1} \max_{\substack{1 \leq j < k \\ k > 0 \text{ or} \\ k < j \leq -1}} \frac{N_v(P_1, P_2)}{D_v(P_1, P_2)}. \quad (6)$$

As a result, two matched pixel pairs should have a convexity measure less than 1 if they straddle the same edge.

Let  $\phi^+(n_x, n_y)$  (or  $\phi^-(n_x, n_y)$ ) represent the angular deviation between  $\vec{E}(n_x, n_y)$  (detected edge orientation at coordinate  $(n_x, n_y)$ ) and  $\vec{E}(n_x + k, n_y + 1)$  (or  $\vec{E}(n_x - k, n_y - 1)$ ). The third feature, edge continuity measure is defined to be

$$c(P_1) = \frac{1}{\pi} \min\{|\phi^+(n_x, n_y)|, |\phi^-(n_x, n_y)|\}. \quad (7)$$

For a valid edge, we assume an edge does not change direction abruptly, and thus  $c(P_1)$  should be smaller than a certain value [4].

We first create synthetic images with known edge information to compute the statistics of the edge feature measures. Two edge model parameters,  $h$  and  $\theta$ , are defined in Fig. 1. We test edges with  $\theta = 0$  to  $360^\circ$ ,  $1^\circ$  apart. The edge orientation  $\theta$  is independent of the edge magnitude  $h$ . Assuming  $h$  is known or detectable, many feature parameters such as edge magnitude, diversity measure and noise power are normalized to  $h$  in our analysis. First, we investigate the bound of the edge diversity measure. As shown in (2), the diversity measure consists of two terms. For an edge obtained by aperture sampling, if  $P_1$  and  $P_2$  are on the same edge,  $\nabla P_1$  and  $\nabla P_2$  should have the same polarity around the local edge region. Consequently, the worst case of this measure occurs when  $\nabla P_2 = 0$  and its diversity measure is  $d(P_1, P_2) = 2|\nabla P_1|$ . That is,  $2|\nabla P_1|$  is the upper bound of the diversity measure for a noise-free edge. Fig. 3 shows the distribution of the diversity measure versus  $|\nabla P_1|$  on the synthetic edge images. Because of the symmetry, the synthetic images are generated with edge declining angle  $\theta$  ranging from  $0^\circ$  to  $90^\circ$  without affecting the results. We observe that this upper bound is too strict in the practical cases, especially when  $|\nabla P_1|$  is larger than  $0.3h$ . As indicated in Fig. 3, the distribution is divided into two regions according to the magnitude of  $g = |\nabla P_1|$  to match the experimental results. The bounds of the two regions are expressed as

$$D(g) = \begin{cases} 2g, & g \leq 0.3h \\ 0.6h, & 0.3h < g. \end{cases} \quad (8)$$

In contrast to the diversity measure, (6) shows that the convexity measure is independent of  $h$ . Two matched pixel pairs should have a convexity measure less than 1 if the edge orientation is correctly detected. Since (6) takes the maximum operation on the index  $j$ , the convexity measure is sensitive to noise disturbance if the edge magnitude  $|\nabla P_1|$  is too small. However, this will not be a critical problem because an

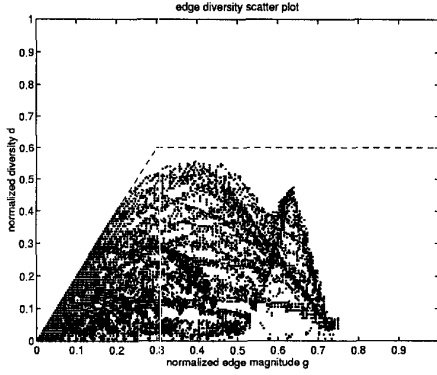


Figure 3: Diversity measure v.s. gradient for the edges.

edge with magnitude less than a certain value is often not considered an edge. The convexity measure should be less than 1 for two matched pixel pairs along the edge orientation. Based on this convex constraint, we conduct the simulation to investigate the missing edge probability (i.e., the probability that the edge orientation of a significant edge is erroneously detected) by using the synthetic images generated in the diversity measure study. Because the existence of an edge is somewhat subjective, it is difficult to obtain the false edge probability (i.e., the probability that an insignificant edge or a smooth area is detected as a significant edge due to the impaired noise). On the other hand, the false edge probability depends strongly on the edge orientation determination algorithm. Fig. 4 shows the effect of the noise power and the edge magnitude threshold  $T_g$  on the missing edge probability. The parameter next to each curve is its corresponding threshold. A pixel pair is determined to cross an edge if its pixel difference is larger than the threshold  $T_g$ . It is obvious that the missing probability equals zero if the test images are noiseless. Increasing the edge magnitude threshold reduces the missing edge probability because the higher magnitude edges can tolerate larger noise. However, the small magnitude edges are not detected if the threshold is set too high.

### 3 Edge Orientation Determination Algorithm

Observing the practical simulation results, the convexity measure is found to be a powerful feature for detecting the edge orientation. Unfortunately, the convexity measure is only available for those sliding pixel pairs located at least two pixels above the anchor pixel pair, as seen in (6). To cope with this drawback, com-

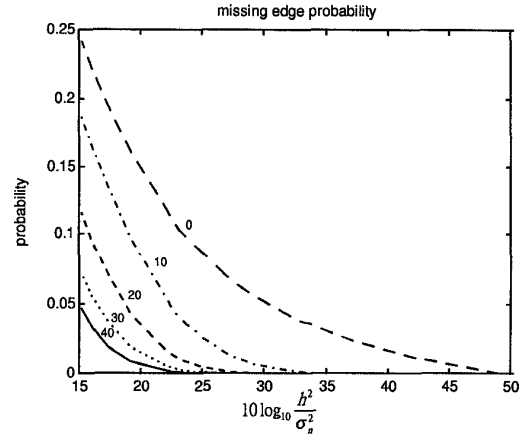


Figure 4: Missing edge probability due to convexity measure.

binning the diversity measure can offer the necessary information to determine the edge orientation for those sliding pixel pairs located less than two pixels from their anchor pixel pairs. As stated earlier, the continuity measure is a global test. Thus, this feature is not useful at the local detection stage. It is merely useful to reduce the false edge probability by post-processing the detected edges after the local stage. For this reason, the whole algorithm is divided into two stages, as shown in Fig. 5.

The first local stage preliminarily examines the edge magnitude of the current anchor pixel pair. If its edge magnitude is larger than a pre-selected threshold  $T_g$ , continue to check the convexity measure for the  $n$ th sliding pixel pair.  $L$  is the total number of the sliding pixel pairs checked on the sliding line for each anchor pixel pair. For those sliding pairs with convexity measure less than 1, the one having the minimum diversity measure is then taken to be the best matched pixel pair if its diversity measure is less than a quantity  $d_{min}$ . In the meantime, the edge orientation at the current anchor pixel pair is found to be a vector  $(K, 1)$  or  $(1, K)$ , depending on the anchor pixel pair is horizontally or vertically oriented. In practice, the quantity  $d_{min}$  is initialized to the diversity bound given in (8). Therefore, we have  $d_{min} = D(|\nabla P_1|)$  as our diversity threshold for a significant edge. Evidently,  $h$  in (8) is an unknown parameter but it can be either detected or set to 255. After completing the local stage for the whole image (i.e., the pixel pair index  $i$  exceeds the total pixel pair number  $Z$  of the image), we proceed to the global stage which uses the conti-

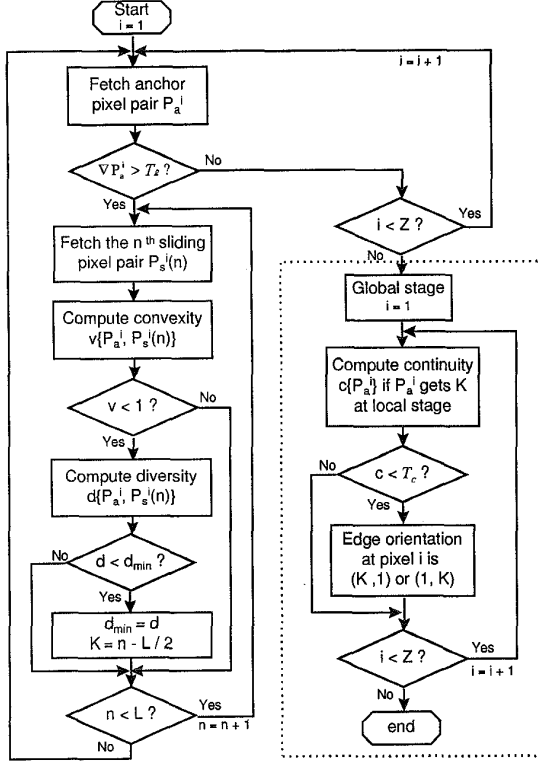


Figure 5: Edge orientation determination algorithm.

nity feature to remove the false edges detected in the local stage. An empirical threshold constant  $T_c$  is chosen to check whether the edge orientation detected for each pixel pair is correct or not.

#### 4 Edge Orientation Map at Subpixel Precision

The detected edge orientation vectors produced by the previous algorithm are confined to integer pixel accuracy. The integer-valued vectors is advantageous for interpolating the digital images for an integer-valued zooming factor. Additional processing is necessary to improve the edge orientation accuracy. Based on the edge profile similarity property of the continuous edge model, we have

$$\mathcal{I}_{h,\theta}(n_x w, n_y w) = \mathcal{I}_{h,\theta}(n_x w + k w, n_y w + w), \quad (9)$$

if  $\tan \theta \geq 1$ . For convenience, we only discuss the horizontal edge profiles because the vertical ones have the same property. Let  $k = K + \delta$  where  $K$  is the nearest integer of  $k$  and expand (9) by Taylor's expansion

along the horizontal axis, we have

$$\mathcal{I}_{h,\theta}(n_x w, n_y w) = \mathcal{I}_{h,\theta}(n_x w + K w, n_y w + w) + \delta \cdot w \frac{\partial \mathcal{I}_{h,\theta}(n_x w + K w, n_y w + w)}{\partial x} + R, \quad (10)$$

where  $R$  is the insignificant remainder terms in the expansion. Neglecting the remainder terms, the discrete representation of (10) is

$$I(n_x, n_y) = I(n_x + K, n_y + 1) + \delta \cdot \frac{\partial I(n_x + K, n_y + 1)}{\partial x}. \quad (11)$$

Approximating the partial derivative by the discrete first-order gradient, the subpixel correction term of the edge orientation vector is approximated by

$$\hat{\delta} = \frac{I(n_x, n_y) - I(n_x + K, n_y + 1)}{\nabla_x I(n_x + K, n_y + 1)}. \quad (12)$$

Thus, the estimated edge orientation angle is expressed as  $\hat{\theta} = \tan^{-1} \frac{1}{K + \hat{\delta}}$ . We now examine the proposed algorithm with subpixel correction on the synthesized images with known orientations. Table 1 summarizes the absolute mean and the root mean square (RMS) of the estimated displacement error  $\tan \theta - \tan \hat{\theta}$ . Without the correction, the estimated orientation displacement error is uniformly distributed between  $-0.5$  and  $0.5$ . As a result, its theoretic mean magnitude is  $0.25$  and RMS is  $0.29$ . Including the correction term (12), the displacement error would be approximately halved in low noise cases, as indicated in Table 1. For high noise cases, their difference is reduced and the correction term becomes unprofitable.

The orientation accuracy can be further improved by a polynomial fit of the image intensity around the anchor pixel pairs. Let the anchor pixel pair and its two adjacent pixels be represented by a polynomial of three degrees, i.e.,  $I(n_x + x, n_y) = p(x) = a_3 x^3 + a_2 x^2 + a_1 x + a_0$ . From the four pixel intensity values, we derive the polynomial coefficients by solving the following linear simultaneous equations:

$$\begin{bmatrix} -8 & 4 & -2 & 1 \\ -1 & 1 & -1 & 1 \\ 0 & 0 & 0 & 1 \\ 1 & 1 & 1 & 1 \end{bmatrix} \begin{bmatrix} a_3 \\ a_2 \\ a_1 \\ a_0 \end{bmatrix} = \begin{bmatrix} I(n_x - 2, n_y) \\ I(n_x - 1, n_y) \\ I(n_x, n_y) \\ I(n_x + 1, n_y) \end{bmatrix}. \quad (13)$$

Expressing (13) in the matrix form, we have  $\mathbf{M} \cdot \mathbf{a} = \mathbf{b}(n_x, n_y)$ . Clearly,  $\mathbf{M}$  is nonsingular and the coefficient vector  $\mathbf{a}$  equals to  $\mathbf{M}^{-1} \mathbf{b}(n_x, n_y)$ . Next we move to the pixels around the sliding pixel pair with an integer displacement  $K$  from its anchor pixel pair.  $K$  is the nearest integer of the actual displacement  $k$  and has already been derived by the previous edge orientation determination algorithm. The pixel intensity value around the sliding pixel pair is thus estimated as:

$$\begin{aligned} & \hat{\mathbf{b}}(n_x + K, n_y + 1) \\ &= \begin{bmatrix} -(d+2)^3 & (d+2)^2 & -(d+2) & 1 \\ -(d+1)^3 & (d+1)^2 & -(d+1) & 1 \\ -d^3 & d^2 & -d & 1 \\ -(d-1)^3 & (d-1)^2 & -(d-1) & 1 \end{bmatrix} \begin{bmatrix} a_3 \\ a_2 \\ a_1 \\ a_0 \end{bmatrix} \end{aligned} \quad (14)$$

Table 1: Mean absolute (MA) and root mean square (RMS) displacement errors of the detected edge orientation.

SNR	noise free		40dB		35dB		30dB		25dB	
	MA	RMS	MA	RMS	MA	RMS	MA	RMS	MA	RMS
no correction	0.25	0.31	0.26	0.32	0.26	0.32	0.27	0.33	0.28	0.35
1st order correction	0.12	0.17	0.13	0.17	0.14	0.18	0.15	0.19	0.18	0.23
polynomial correction	0.09	0.13	0.09	0.13	0.10	0.14	0.12	0.15	0.15	0.19

In the ideal case,  $\hat{\mathbf{b}}(n_x + K, n_y + 1) = \mathbf{b}(n_x + K, n_y + 1)$  if  $d = \delta$ . Therefore, the correction term  $\hat{\delta}$  should take the  $d$  value which minimizes the mean squared error

$$J = \|\mathbf{b}(n_x + K, n_y + 1) - \hat{\mathbf{b}}(n_x + K, n_y + 1)\|. \quad (15)$$

$J$  is convex with respect to the  $d$  parameter since the intensity profiles around the two pixel pairs are monotonically increasing or decreasing if they have convexity measure less than 1. As indicated in Table 1, the accuracy of the edge orientation is further improved by the polynomial fit method.

## 5 Simulation Results

As shown in Fig. 6(a), a test image composed of four pictures has been used in our experiments. They have different graphical characteristics. The first picture is a Chinese letter which has many oblique edges. The second picture is further composed of four small pictures, including two pictures having letters on shading background and two texture pictures. The third and the fourth pictures are clipped from the “Lena” and the “Pepper” pictures, respectively. Fig. 6(b) shows the edge orientation map of the test image using the proposed algorithm. In this example the edge magnitude threshold  $T_g$  is set to 20 and the edge angle threshold  $T_c$  is set to  $0.2\pi$ . In Fig. 6(b), the horizontal and the vertical edges are marked by white color and gray color, respectively.

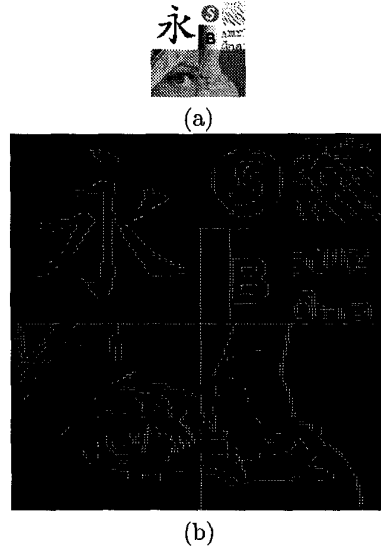
## 6 Conclusions

In this paper, we propose an edge orientation determination method based on several local and global edge properties. The orientation vector candidates of the detected edgel are chosen by a pixel pair matching method. Three measures are designed to detect edges and determine their orientation vectors. The edge orientation precision is further improved by an additional subpixel estimation step.

## References

- [1] E. P. Lyvers and O. R. Mitchell, “Precision edge contrast and orientation estimation,” *IEEE Trans. on Pattern Analysis and Machine Intelligence*, vol. 10, no. 6, pp. 927-937, Nov. 1988.

Figure 6: Edge orientation determination results: (a) original image, and (b) its edge orientation map.



- [2] H. -C. Ting and H. -M. Hang, “Edge preserving interpolation of digital images using fuzzy inference,” *Journal of Visual Communication and Image Representation*, vol. 8, no. 4, pp. 338-355, Dec. 1997.
- [3] K. Jensen and D. Anastassiou, “Subpixel edge localization and the interpolation of still images,” *IEEE Trans. Image Processing*, vol. 4, pp. 285-295, Mar. 1995.
- [4] P. H. Gregson, “Using angular dispersion of gradient direction for detecting edge ribbons,” *IEEE Trans. on Pattern Analysis and Machine Intelligence*, vol. 15, no. 7, pp. 682-696, Jul. 1993.